Modes of Shock-Wave Oscillations on Spike-Tipped Bodies

Wladimiro Calarese* and Wilbur L. Hankey†
Air Force Wright Aeronautical Laboratories, Wright-Patterson Air Force Base, Ohio

The phenomenon of self-excited shock oscillations on a spike-tipped body at Mach 3 is investigated. Various modes of shock oscillations are observed. For some spike lengths, the shock oscillations are symmetric. For other spike lengths, the shock structure oscillates asymmetrically with respect to the spike's axis. In this case, experimental evidence confirms the presence of standing rotational waves on the body face and spike. Spike configurations resulting in stable shock systems are also observed. Holography and interferometry are used to obtain a detailed flow visualization.

Nomenclature

c	= complex wave propagation speed in free shear layer, $= c_r + ic_i$
F1,F2,F3	= high-response transducers (Kulites)
f	= frequency
h	= enthalpy
L	= spike length
m,n	= mode numbers (integers)
P	= period of fundamental frequency
p	= pressure
R	= cross correlation (cross covariance), e.g., $R(\tau) = p'(\text{F1},t)p'(\text{F2},t+\tau)$
r,θ,ϕ	= spherical coordinates
t	= time
u,v,w	= velocity components
α	= wave number, $2\pi/\lambda$ (longitudinal)
λ	= wavelength
ρ	= density
σ_1	= phase angle
τ	= time increment
ϕ_1,ϕ_2,ϕ_n	= phase angles
ω	= $(2\pi f)$ frequency

Superscripts

$(\ )'$	= fluctuating values
$(\ \bar{}\ )$	= mean values
$(\ \hat{}\ )$	= amplitudes

I. Introduction

THE phenomenon of self-excited shock oscillations on spike-tipped bodies of revolution has been studied considerably in past years[1-17] because of the harmful effect caused to vehicles by excessive noise levels and structural loadings. This fluid dynamic instability is known as "buzz." Buzz can occur on supersonic inlets of jet engines, on blunt bodies with drag reducing spikes, on ablating re-entry vehicles, etc. In the past, it was believed that the shock oscillated axially in a symmetric fashion with respect to the spike, but there is evidence that the shock motion can be asymmetric for certain configurations and flow conditions.[1-8, 10-12] In addition, different modes of instability might occur for different spike lengths, i.e., the shock might wave or undulate laterally with respect to the spike,[1,9,16] or it might rotate around the spike.[8]

Presented as Paper 83-0544 at the AIAA 21st Aerospace Sciences Meeting, Reno, Nev., Jan. 10-13, 1983; received Feb. 2, 1983; revision received March 7, 1984. This paper is declared a work of the U.S. Government and therefore is in the public domain.

*Aerospace Engineer. Member AIAA.
†Senior Scientist. Member AIAA.

The present work has been performed to investigate in detail the various aspects of the shock structure of the buzzing phenomenon on spike-tipped bodies. In particular, theoretical analysis and experimental evidence are used to justify the hypothesis that standing rotational waves are present on the spike and body face for some spike lengths.

II. Mechanism of Shock Oscillations

The mechanism of shock oscillations has been illustrated by many researchers.[1-17] A common explanation of the flowfield is: for a given spike length and shoulder bluntness, if the flow just outside the separated shear layer approaching the body's shoulder can be turned by an attached conical shock, then the shock structure is stable since an equilibrium condition is reached between escaping and recirculating flows in the separated region, and no oscillations occur (Fig. 1a); if the turning angle of the flow is too large to be accomplished by an attached conical shock, a detached strong shock is generated which pumps high-pressure flow from the reattachment region at the body's face into the recirculating region of the separated shear layer (Fig. 1b). The high-pressure flow pushes the shock structure upstream relieving the back pressure. A strong detached bow shock results at the spike tip (Fig. 1c). When this occurs, the flow behind the bow shock can escape around the body's shoulder and the shock collapses downstream. This system is unstable and the oscillations continue. This flow pattern has been compared and found to be consistent with the numerical results of Ref. 10.

Some researchers believe that the main reason for the shock oscillations lies in the shear layer reattachment conditions at the body's face. Although this describes the flow process, the authors believe it does not describe the true cause of the instabilities. A complete explanation of spike buzz must include three necessary conditions for self-excited shock oscillations to occur.[2] They are the presence of a shear layer with an inflection point in the velocity profile, which is inherently unstable, a reflecting surface (the body's shoulder) which feeds back pressure waves, and the appropriate spike length to permit in-phase reflection of these waves. If these conditions are met, resonance occurs and selective amplification of disturbances takes place until a limit cycle is reached. All three conditions are therefore crucial.

It may be interesting to compare the fluid dynamic oscillator (just discussed) with an electronic oscillator (Fig. 2). The gain of the system is

$$\text{Gain} = A/(1 - AB)$$

where A is the amplifier and B the feedback. The existence of a frequency for which the return ratio AB equals unity is a sufficient condition for a self-excited oscillation to occur.

However, self-excited oscillations will result only for very specific phase relationships as mentioned above.

III. Mode, Frequency, and Shape Determination

It is well known that a two-dimensional flow is unstable when small disturbances are present, as in the case of a shear layer which has an inflection point in its velocity profile. Rayleigh[18] showed that these disturbances are greatly amplified over a limited frequency range. It is then plausible to assume that the same conditions can be encountered in an axisymmetric flowfield. In this case, it is hypothesized that the disturbances in a separating shear layer could trigger the onset of shock oscillations with various modes. To examine the different modes of oscillation it is informative to analyze the possible forms of pressure waves that can exist on the spike. Consider a pair of downstream traveling waves with origin at the spike tip ($r=0$) rotating in opposite directions of equal frequency and intensity.

$$p_1' = 2\hat{p}\exp[i\alpha(r-ct)]\cos n\phi \tag{1}$$

Now consider another pair of opposite rotating upstream traveling waves with the origin at $r=L$

$$p_2' = 2\hat{p}\exp[-i\alpha(r-L+ct)]\cos n\phi\exp[i\sigma_1] \tag{2}$$

where σ_1 is an unknown phase angle. Adding these together produces the combined pressure fluctuation

$$p' = p_1' + p_2' = 2\hat{p}\exp[-i\omega t]\cos n\phi\{\exp[i\alpha r] + \exp[-i\alpha(r-L)+i\sigma_1]\} \tag{3}$$

Application of appropriate r boundary conditions at the end points will determine both α and σ_1. Considering a symmetric mode shape for which $\partial p'/\partial r = 0$ (antinode) at $r=0$ and L, we obtain

$$p' = 4\hat{p}e^{-i\omega t}\cos n\phi\cos\alpha r \tag{4}$$

$$\alpha = m\pi/2L \quad (m \text{ even}) \tag{5}$$

$$\sigma_1 = \alpha L \tag{6}$$

$$f = \frac{\alpha c_r}{2\pi} = \frac{mc_r}{4L} \quad (m \text{ even}) \tag{7}$$

Alternatively, let us also consider antisymmetric boundary conditions $p'(r=0)=0$ (node); $\partial p'/\partial r\,(r=L)=0$ (antinode)

$$p' = 2\hat{p}e^{-i\omega t}\cos n\phi[2i\sin\alpha r] = 4i\hat{p}e^{-i\omega t}\cos n\phi\sin\alpha r \tag{8}$$

$$\alpha = m\pi/2L \quad (m \text{ odd}) \tag{9}$$

$$\sigma_1 = \alpha L \tag{10}$$

In all cases, $f = mc_r/4L$, $\alpha = m\pi/2L$, $f = \omega/2\pi$. The real part of the pressure fluctuation is:

For the symmetric case, m = even

$$p' = 4|\hat{p}|\cos\omega t\cos n\phi\cos\alpha r \tag{11}$$

For the antisymmetric case, m = odd

$$p' = 4|\hat{p}|\sin\omega t\cos n\phi\sin\alpha r \tag{12}$$

where the value of n has not yet been identified for either case. At this point an interpretation of the different modes should be presented (Fig. 3). At the spike tip ($r=0$) the derivatives of the pressure and peripheral velocity fluctuations, p' and w', with respect to the azimuthal direction ϕ, must vanish in order to prevent a nonphysical singularity from occurring. This may be obtained under two circumstances: 1) $w'=0$ for all r values, or no rotation, $n=0$; 2) $w'=0$ ($r=0$) node only at the spike tip, $n\neq 0$, rotation possible. Case 1 occurs for the symmetric mode (m = even), no rotation. Equation (11) becomes

$$p' = 4|\hat{p}|\cos\omega t\cos\alpha r \tag{13}$$

Case 2 occurs for the antisymmetric mode (m = odd), rotation [Eq. (12)]. Based upon the above argument, it is plausible to formulate the following hypothesis: A secondary separation in the shear layer creates a sudden burst of pressure on one side of the spike causing a pressure fluctuation to be higher than on the other side of the spike. The pressure wave is an odd-mode wave which allows for rotation to occur. Under this condition the high-response transducers of the frustum face would be anticorrelated (180 deg out of phase). The rotational waves excited by the shear layer separation must travel in both azimuthal directions in a helicoidal fashion. This produces standing rotational waves of integer wavelength, which are periodic and reinforced. All other waves interfere and are damped. Therefore, it is again plausible to state that the fundamental frequency for rotational antisymmetric waves (odd) would be one-half the fundamental frequency of the nonrotating symmetric ones (even). The same conditions would also justify the occurrence of "rocking" shock oscillations alternating from opposite sides of the frustum, as suggested by Refs. 1 and 12. To explore these hypotheses, an experimental program was conducted to investigate the frequency and phase relationship of the different modes.

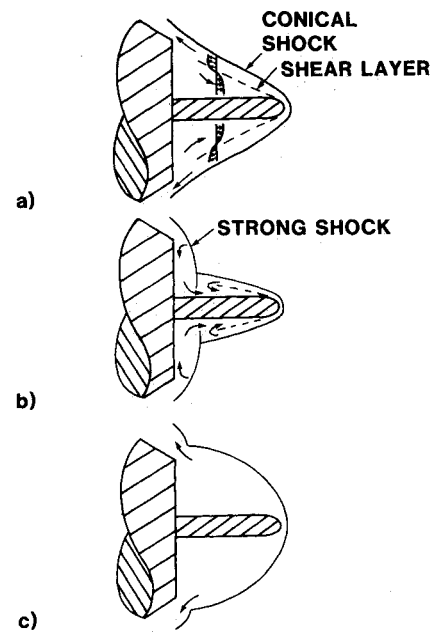

Fig. 1 Steady and unsteady shock system.

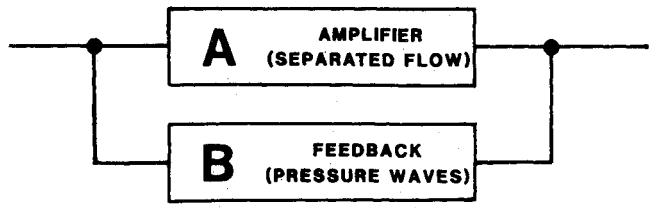

Fig. 2 Oscillator with feedback.

IV. Equipment and Test Description

The experiments were performed at the Trisonic Gasdynamic Facility of the Air Force Wright Aeronautical Laboratories. A description of the facility is given in Ref. 19. Tests were conducted at Mach 3 and a unit Reynolds number of 7×10^6/m on a cone frustum axisymmetric model with a retractable spike placed at zero angle of attack (Fig. 4). The spike and the frustum face were equipped with high-response transducers (Kulites). An rms meter and a Fourier analyzer were used during the tests to record pressure fluctuations, power spectral densities, and cross correlations. The flow visualization was accomplished using holography, with the reference beam passing through the test section, to obtain high-resolution photography, and interferometry and high-speed cameras capable of 44,000 frames/s to obtain slow motion movies. For the holography process, a 3 mJ ruby pulse laser was used capable of pulses of 30 ns, while a 15 mW helium-neon continuous-wave laser was used for the interferometry.

V. Experimental Results

Shock Structure

Some features of the shock structure were previously investigated in Refs. 10 and 11. Depending on the spike length, the flow may be steady or unsteady resulting in either a stable or unstable shock structure. Experimental data show that the stable shock configurations occur for spike lengths corresponding to

$$L \leq 13 \text{ mm} \quad \text{and} \quad L \geq 44 \text{ mm}$$

while the unstable shock structures develop for spike lengths between 20 and 43 mm (Fig. 5). Low levels of pressure fluctuations indicate a stable configuration, while high levels show an unstable shock structure. The theory outlined in Ref. 10 involved the numerical solution of the Navier-Stokes equations by a time-dependent algorithm devised by MacCormack.[20] The theoretical results obtained for a spike length of 12.7 mm show a stable shock configuration and are consistent with the experiment (Fig. 6). Power spectral densities at these lengths indicate primarily broadband noise and no major peaks at any frequency. No shock oscillations occur in any direction. An illustration of an unstable shock configuration is given in Fig. 7. It shows in detail the unstable shock structure and flowfields for a spike length of 30 mm obtained with outward motion. Two successive shock positions for two pulses 200 μs apart are depicted; the conical shock which intersects the strong detached shock near the body's shoulder is pushed upstream and becomes a strong detached bow shock. In this particular oscillating position the "conical" shock exhibits a quasiparabolic shape.

The unstable shock structure has two different modes of instability which correspond to different spike lengths; even- or odd-frequency modes of oscillation. The Strouhal number (fD/U_∞) based on body face diameter, freestream velocity, and fundamental frequency of oscillations is 0.22. A close examination of Fig. 5 shows that the intensity of the pressure fluctuations increases dramatically for spike lengths between 20 and 42 mm, signifying that shock oscillations take place. The intensity of the fluctuations is higher on one side of the frustum face (Kulite F3). A hysteresis phenomenon occurs when the spike is retracted. It is attributed to the fact that the shock configuration tends to conserve its state; once the shock oscillations are induced by the spike outward motion, they sustain themselves even when the spike reaches a length which would require the onset of a stable configuration; similarly, when the spike is retracted, the existing stable shock configuration tends to remain unchanged for spike lengths which would require the onset of the shock oscillations.

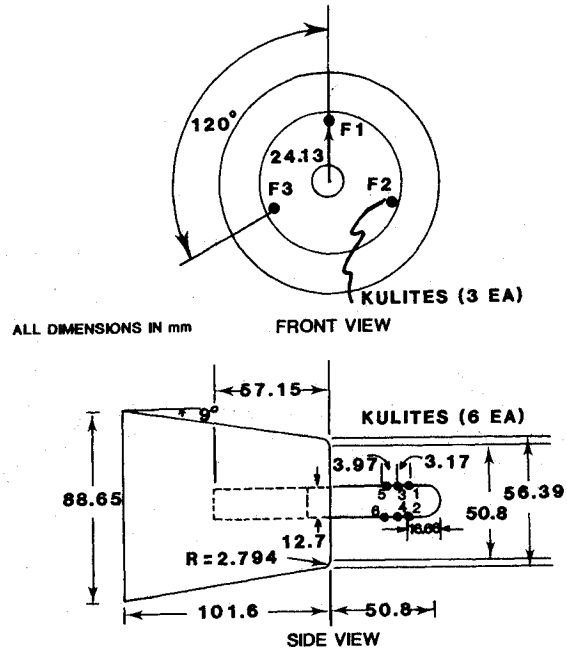

Fig. 4 Spike-tipped model used during testing.

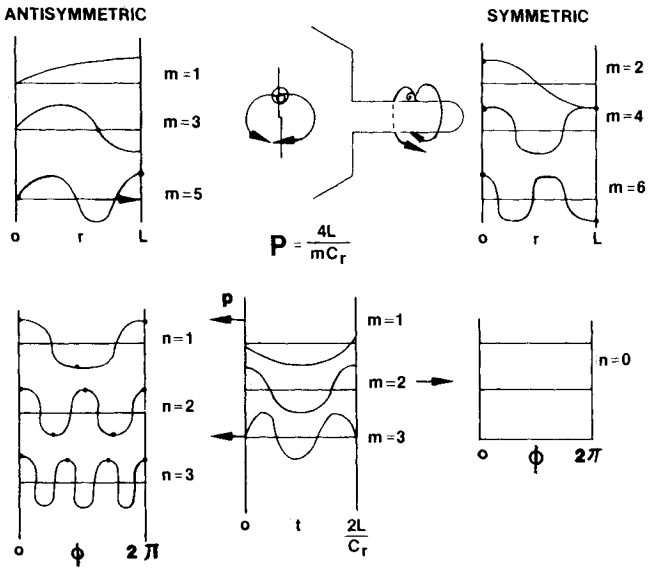

Fig. 3 Modes of oscillations of pressure waves.

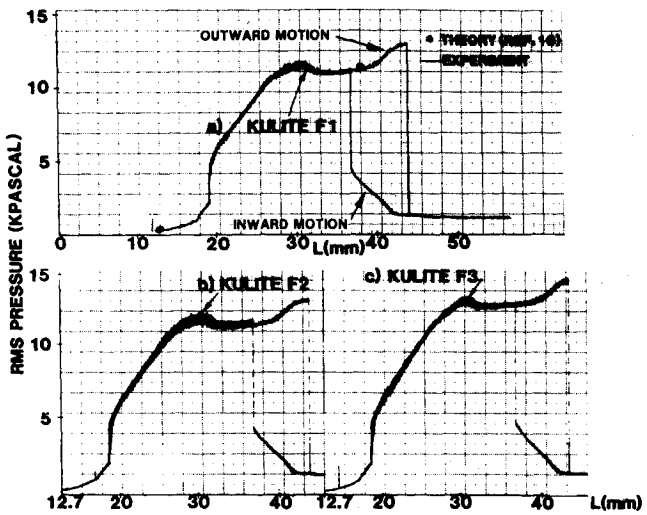

Fig. 5 Pressure oscillation vs spike length.

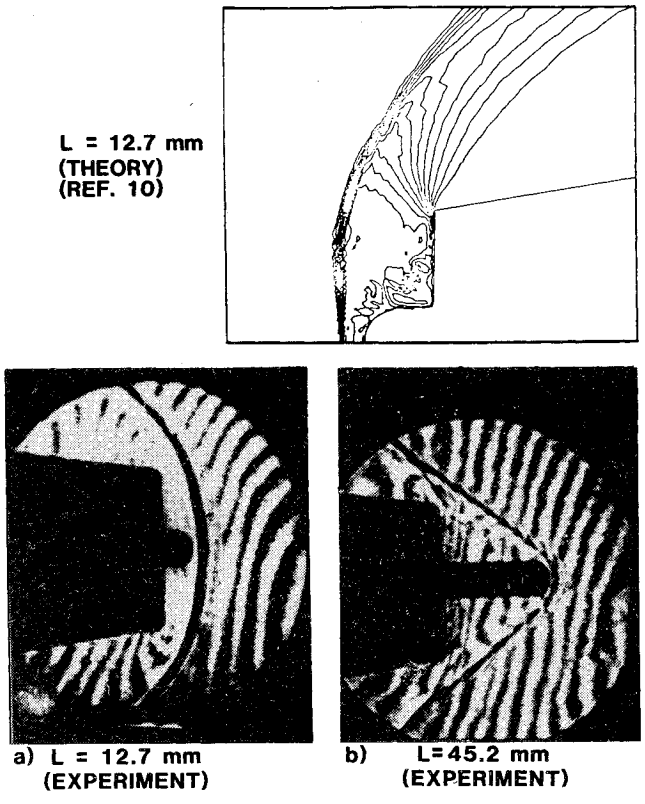

Fig. 6 Stable shock pattern for different spike lengths.

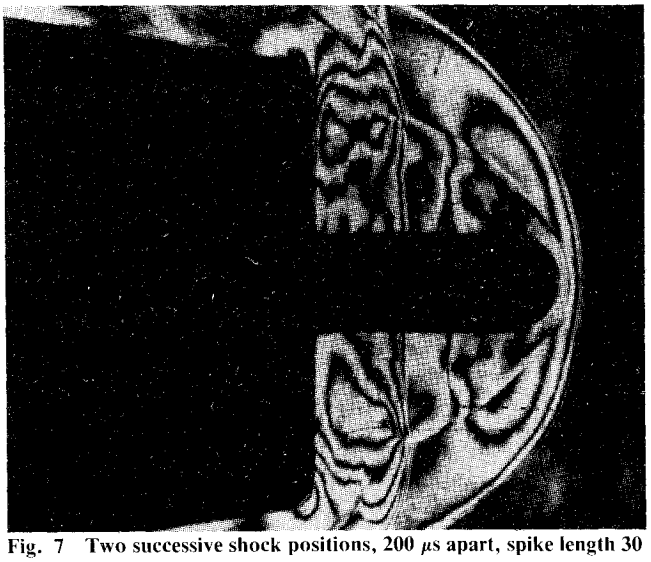

Fig. 7 Two successive shock positions, 200 μs apart, spike length 30 mm.

At $L=20.32$ mm, the shock oscillations just begin to take place and the intensity of the pressure oscillations caused on the frustum face is not too high (see Fig. 5). The primary mode (even mode) associated with axial shock oscillations has a fundamental frequency of about 2800 Hz and higher harmonics, as shown by the power spectral density plot of Fig. 8 (the frequency of oscillations decreased slightly with spike length down to 2700 Hz, but throughout the paper the 2800 Hz frequency value was used for simplicity). This oscillating wave is modulated with another wave of about half the frequency (odd mode). Cross correlations of the high-response transducers on the frustum face show that the modulating wave is correlated (in phase) with the primary mode wave on one side of the frustum face and its amplitude is low (check the small high-low undulations of the wave peaks for Kulites F1-F2 on Fig. 9a), while it is anticorrelated (180 deg out of phase) on the other side of the frustum face and its amplitude is high (check the corresponding large low-high undulations of the wave peaks for Kulites F1-F3 and F2-F3 in Figs. 9b and 9c). The varying amplitude of the modulating wave shows that an incipient asymmetry takes place in the shock structure. The interpretation of the wave peaks of the cross correlations is presented in the Appendix.

At $L=25.4$ mm, a similar result is obtained. Power spectral densities taken at the frustum face and on the spike (Figs. 10 and 11) show that the shock system oscillates axially at a fundamental frequency of 2800 Hz and an odd-mode wave with a frequency of 1400 Hz is present, but now the intensity of the pressure oscillations on the frustum face is much higher (see Fig. 5). The odd-mode wave is associated with an asymmetric splitting of the shock which can be clearly observed in every other cycle of oscillations (Fig. 12c and 12d′, which are frames of high-speed interferometry movies). This asymmetric splitting is believed to be generated by a secondary separation which causes a sudden burst of pressure on one side of the spike. Cross correlations show that the odd-mode wave modulates the even-mode wave. The high-response transducers on each side of the spike (Fig. 13a) are in phase (high-low undulations), while the transducers on opposite sides of the spike and on the frustum face are out of phase (low-high undulations, Fig. 13b). Therefore, the odd-mode disturbance, with asymmetric shock splitting, generates two distinct counter-rotating waves about the spike which proceed downstream onto the frustum face. At the frustum face the cross correlations show that the odd-mode wave slightly modulates the primary-mode wave on one side of the frustum face while modulating it strongly on the other side. This is consistent with the postulation of Sec. III. The modulations on the spike show the presence of rotating waves. The different modulations on the frustum face indicate that the disturbance is highly asymmetric and directed toward half of the frustum face, but certainly cannot justify the explanation that the shock system flaps from one side of the frustum to the other. The authors of Refs. 1 and 12 believed that the odd-

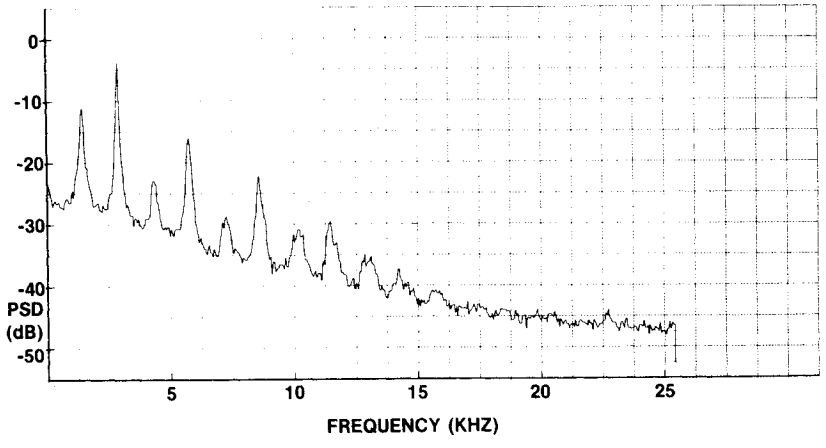

Fig. 8 Power spectral density, spike length 20.32 mm, Kulite F1.

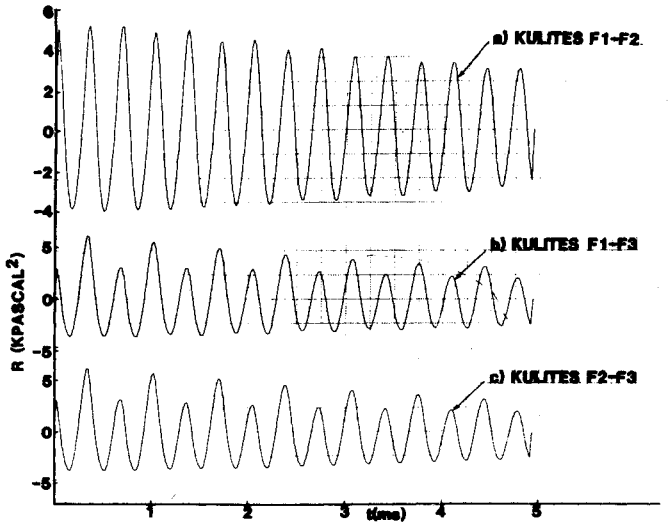

Fig. 9 Cross correlation, spike length 20.32 mm (outward motion).

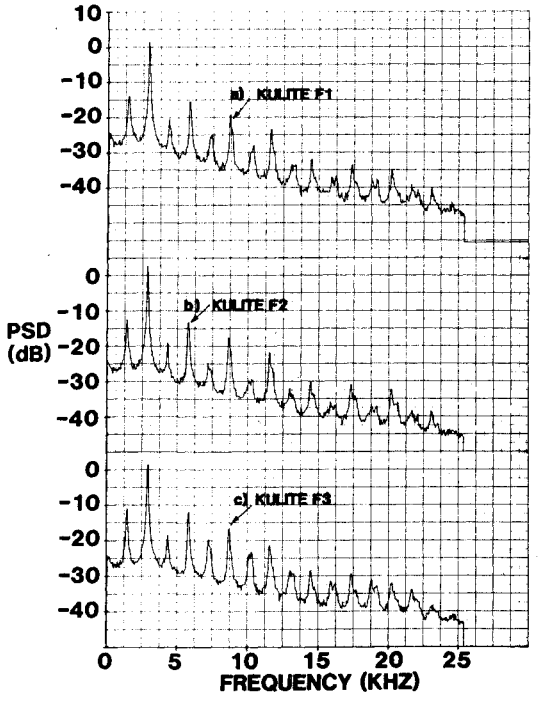

Fig. 10 Power spectral density, spike length 25.4 mm.

mode wave was a rocking wave which gave rise to an asymmetric pressure distribution on the body face. Close scrutiny of the high-speed movies showed no evidence at all of a rocking motion of the shock from one side of the frustum to the other. The authors of Ref. 8 speculated that this odd-mode wave might rotate about the spike completing one revolution for every two cycles of the axial oscillations. However, they could not explain the origin and sense of the rotation. The experimental evidence obtained so far does not support a rotational bias in one direction around the spike. If a rotational wave were present, the response of the three Kulites, which are positioned on the frustum face 120 deg apart from each other, should be about 120 deg out of phase. However, examination of the experimental evidence does not support this. Fourier analyzer data collected on the phase relation among the frustum face transducers for the primary- and secondary-mode frequencies showed that, at the primary oscillation frequency, about 2800 Hz, the transducers were practically in phase, being only less than 10 deg off. At the secondary frequency, about 1400 Hz, they were anticorrelated, i.e., out of phase between 170 and 180 deg. A check of the coherence function which gives the linear dependency between input and output signals showed perfect coherence (1.0) for the primary frequency, while a coherence level of 0.5 to 0.9 was obtained for the secondary frequency. The diminished coherence probably resulted from the contributions of extraneous measurement noise since the secondary mode exhibited a low amplitude, close to the noise level. Since the energy peak of the secondary mode was not sharp but had instead a finite bandwidth, phase information for 1400 and 1450 Hz was obtained. It was found that, at one frequency, the transducers were about 180 deg out of phase while, at the other frequency, they were about -180 deg out of phase. This can be construed as further proof that the asymmetric shock oscillations generate rotational waves in both directions about the spike, creating a standing rotational wave as postulated in Sec. III.

At $L=38.1$ mm, produced by traversing the spike outwardly (shown in the hysteresis area of Fig. 5 as the upper branch of the curve where high-intensity oscillations occur), the shock system oscillates axially at a frequency of 2800 Hz (Figs. 14 and 15) and higher harmonics. The odd-mode wave at 1400 Hz frequency is not present and the oscillations are perfectly symmetric. The high-response transducers on the spike and the frustum face show no modulation and negligible sinusoidal damping, and are perfectly correlated. Figure 16, taken from Ref. 10, shows the symmetric shock oscillations and a comparison with theoretical results.

At $L=38.1$ mm, produced by traversing the spike inwardly (lower branch of the curve of Fig. 5 where low-intensity oscillations occur), no axial shock oscillations are present,

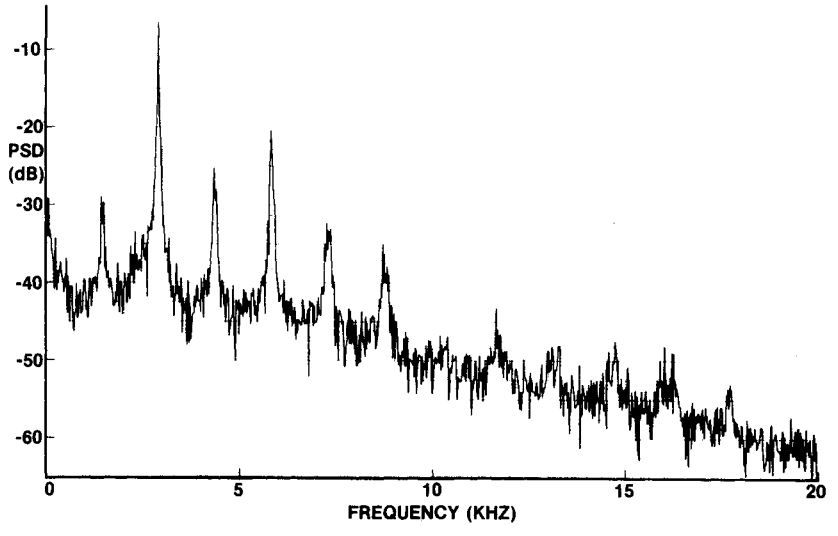

Fig. 11 Power spectral density, spike length 25.4 mm, Kulite 3.

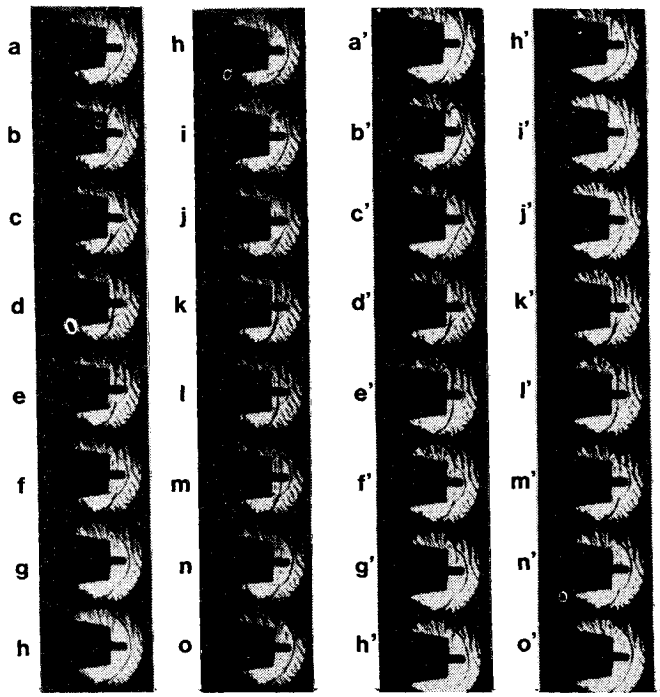

Fig. 12 Shock wave oscillations, four cycles, recorded at 22,000 frames/s, $M = 3.0$, spike length 25.4 mm.

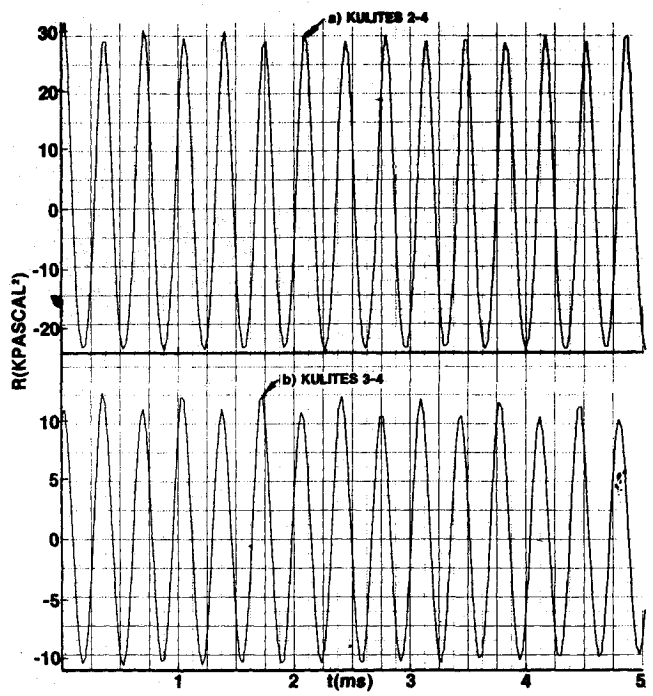

Fig. 13 Cross correlation, spike length 25.4 mm.

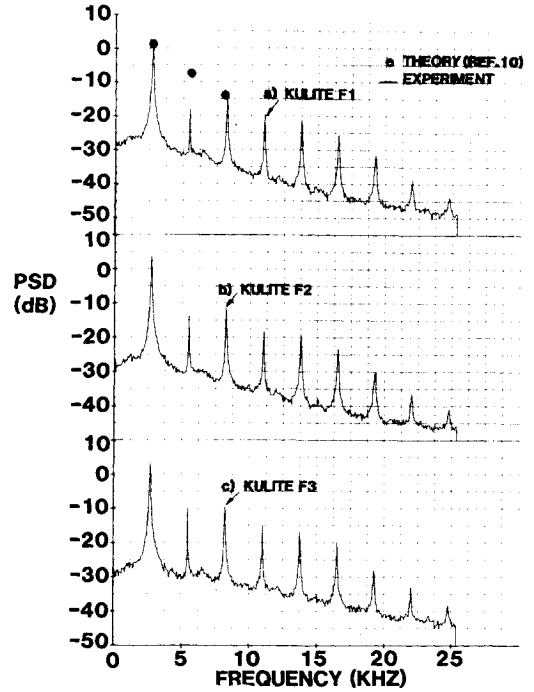

Fig. 14 Power spectral density, spike length 38.1 mm, Kulites F1, F2, F3 (outward motion).

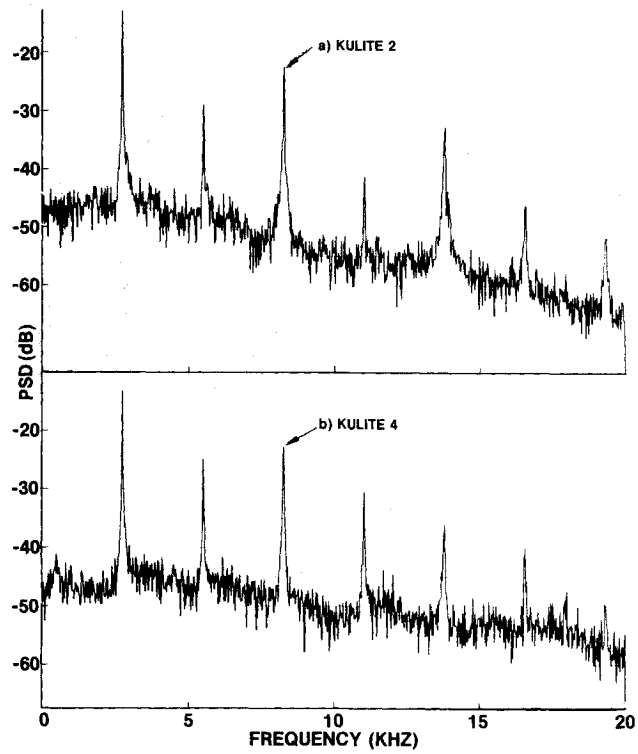

Fig. 15 Power spectral density, spike length 38.1 mm, Kulites 2 and 4 (outward motion).

only a mild symmetric waving of the shock occurs. The oblique shock system undulates laterally at low intensity and changes shape from concave to convex and vice versa. This mild undulation persists for longer spike lengths outside the hysteresis area, as also reported by Refs. 9 and 16. The related power spectral density shows a shift in the oscillation frequency, from 2800 Hz to approximately 3500 Hz (Fig. 17a), which is due to the different type of shock motion. Reducing the spike length further to 33.02 mm, which is outside the hysteresis area, the fundamental frequency reverts back to 2800 Hz (Fig. 17b). The cross correlations at $L = 38.1$ mm for inward motion are not modulated and confirm the absence of an odd-mode wave.

VI. Conclusions

An experimental investigation has been performed to investigate the various shock systems occurring on a spike-tipped body at Mach 3. An analysis of the various modes of self-sustained shock oscillations has been performed and compared to experimental results. The conclusions are:

1) The various shock systems existing on the spike-tipped body tested can be stable or unstable depending on the spike length.

2) When the unstable shock configuration occurs, the shock may oscillate axially in a symmetric or asymmetric fashion which also depends on the spike length. In the

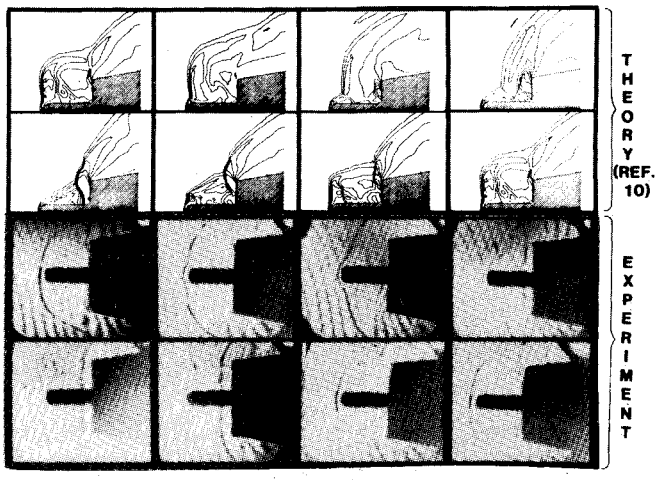

Fig. 16 Theoretical and experimental shock oscillations for a spike length of 38.1 mm, one cycle, $M=3$ (outward motion).

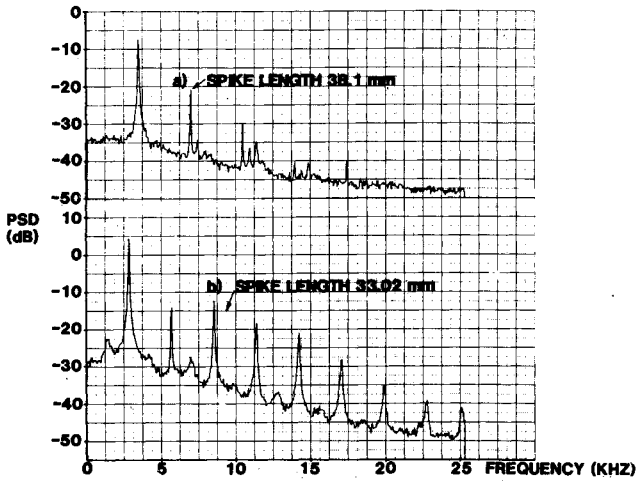

Fig. 17 Power spectral density, Kulite F1 (inward motion).

asymmetric case, experimental results show that a secondary wave (odd mode), half the frequency of the primary wave (even mode), modulates the primary wave and is out of phase with respect to the primary wave. The secondary wave is considered to be a standing rotational wave.

3) A hysteresis phenomenon occurs when the spike is extended or retracted between a length of 36 and 43 mm. For the outward motion the shock oscillations exhibit much higher intensity than for the inward motion and the frequency and type of oscillations are different. For the inward motion, the longitudinal shock oscillations change into shock waving. Some shock waving persists for longer spike lengths, outside the hysteresis area.

Appendix: Interpretation of Cross-Correlation Signals

It is useful to analyze the cross correlations of the high-response transducers' signals in order to confirm the phase relationship of the transducers.

Consider two signals (only ac level)

$$p_1'(t)=\sum_{n=1}^{\infty}\left(a_n\sin\frac{n\pi t}{P}+b_n\cos\frac{n\pi t}{P}\right) \tag{A1}$$

$$p_2'(t)=\sum_{n=1}^{\infty}\left(A_n\sin\frac{n\pi t}{P}+B_n\cos\frac{n\pi t}{P}\right) \tag{A2}$$

These signals are composed of commensurate frequencies, i.e., n=integer, P=fundamental frequency period. The cross

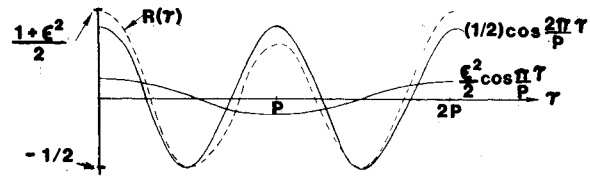

Fig. A1 Cross correlation, case I, zero phase shift.

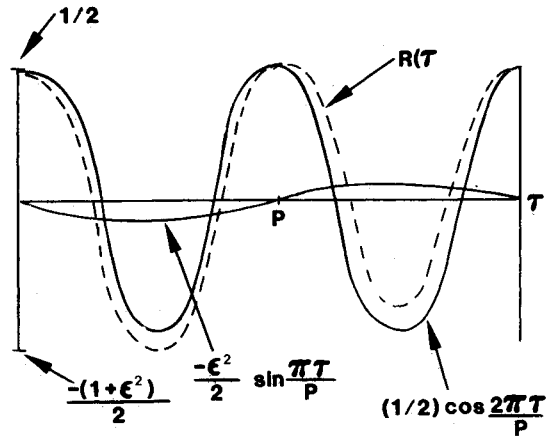

Fig. A2 Cross correlation, case II, 90 deg phase shift.

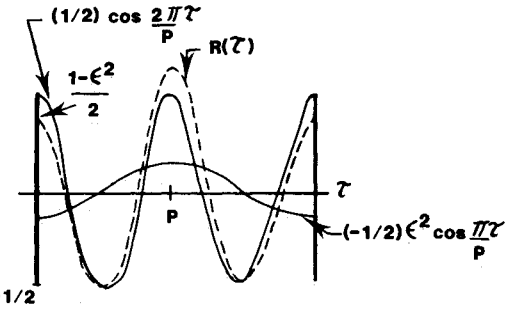

Fig. A3 Cross correlation, case III, 180 deg phase shift.

correlation (time) is defined as follows:

$$R(\tau)=\overline{p_1'(t)p_2'(t+\tau)} \tag{A3}$$

$$\begin{aligned}\overline{p_1'p_2'}(\tau)&=\frac{1}{P}\int_0^P\sum\left(a_n\sin\frac{n\pi t}{P}+b_n\cos\frac{n\pi t}{P}\right)\\&\times\sum\left(A_n\sin\frac{n\pi(t+\tau)}{P}+B_n\frac{n\pi(t+\tau)}{P}\right)dt\\&=\frac{1}{P}\int_0^P\sum a_n\left(A_n\cos\frac{n\pi\tau}{P}-B_n\sin\frac{n\pi\tau}{P}\right)\sin^2\frac{n\pi t}{P}\,dt\\&+\frac{1}{P}\int_0^P\sum b_n\left(A_n\sin\frac{n\pi\tau}{P}+B_n\cos\frac{n\pi\tau}{P}\right)\cos^2\frac{n\pi t}{P}\,dt\end{aligned} \tag{A4}$$

since the integral of the terms including $\sin(n\pi t/P)\cos(n\pi t/P)$ is equal to zero. Therefore,

$$\begin{aligned}R(\tau)=\overline{p_1'p_2'}(\tau)&=\sum\frac{a_n}{2}\left(A_n\cos\frac{n\pi\tau}{P}-B_n\sin\frac{n\pi\tau}{P}\right)\\&+\sum\frac{b_n}{2}\left(A_n\sin\frac{n\pi\tau}{P}+B_n\cos\frac{n\pi\tau}{P}\right)=\frac{1}{2}\sum(a_nA_n+b_nB_n)\\&\times\cos\frac{n\pi\tau}{P}+\frac{1}{2}\sum(b_nA_n-a_nB_n)\sin\frac{n\pi\tau}{P}\end{aligned} \tag{A5}$$

Equation (A5) can be put in the following form:

$$R(\tau)=\sum_{n=1}^{\infty}\hat{R}_n\cos\left(\frac{n\pi\tau}{P}-\phi_n\right) \tag{A6}$$

$$\tan\phi_n=\frac{b_nA_n-a_nB_n}{a_nA_n+b_nB_n} \tag{A7}$$

$$\hat{R}_n=[\,\tfrac{1}{4}(a_nA_n+b_nB_n)^2+\tfrac{1}{4}(b_nA_n-a_nB_n)^2\,]^{1/2} \tag{A8}$$

$$R(\tau)=\sum_{n=1}^{\infty}\hat{R}_n\left(\cos\frac{n\pi\tau}{P}\cos\phi_n+\sin\frac{n\pi\tau}{P}\sin\phi_n\right) \tag{A9}$$

Case I, zero phase shift (Fig. A1)

$$\phi_1=0\text{ deg},\quad \phi_2=0\text{ deg}$$

$$b_nA_n-a_nB_n=0,\quad b_n=B_n=0,\quad a_n=A_n$$

Let $a_1=\epsilon$, $a_2=1$, $a_{n>2}=0$ since only two waves are considered

$$R(\tau)=\frac{1}{2}\sum_{n=1}^{2}a_n^2\left(\cos\frac{n\pi\tau}{P}\cos\phi_n\right)=\frac{\epsilon^2}{2}\cos\frac{\pi\tau}{P}+\frac{1}{2}\cos\frac{2\pi\tau}{P} \tag{A10}$$

Note that the modulation occurs on top of the wave. The bottom of the wave is unaltered. For 0 deg phase shift, high-low peaks occur at $\tau=nP$.

Case II, 90 deg phase shift (Fig. A2)

$$\phi_1=90\text{ deg},\quad \phi_2=0\text{ deg}$$

$$a_1A_1+b_1B_1=0,\quad b_1=A_1=0,\quad a_1=B_1,\quad a_1=\epsilon$$

$$b_2A_2-a_2B_2=0,\quad b_2=B_2=0,\quad a_2=A_2=1$$

$$R(\tau)=\frac{1}{2}\sum_{n=1}^{2}(-1)^n a_n^2\left(\cos\frac{n\pi\tau}{P}\cos\phi_n+\sin\frac{n\pi\tau}{P}\sin\phi_n\right)$$

$$=-\frac{\epsilon^2}{2}\sin\frac{\pi\tau}{P}+\frac{1}{2}\cos\frac{2\pi\tau}{P} \tag{A11}$$

Note that the modulation occurs at the bottom of the wave. The top of the wave is unaltered. For 90 deg phase shift, low-high peaks occur at $\tau=nP/2$, n odd.

Case III, 180 deg phase shift (Fig. A3)

$$\phi_1=180\text{ deg},\quad \phi_2=0\text{ deg}$$

$$b_nA_n-a_nB_n=0,\quad b_n=B_n=0,\quad a_n=A_n,\quad a_1=\epsilon,\quad a_2=1$$

$$R(\tau)=\frac{1}{2}\sum_{n=1}^{2}a_n^2\left(\cos\frac{n\pi\tau}{P}\cos\phi_n\right)=-\frac{1}{2}\epsilon^2\cos\frac{\pi\tau}{P}+\frac{1}{2}\cos\frac{2\pi\tau}{P} \tag{A12}$$

Note that the modulation occurs on top of the wave. The bottom of the wave is unaltered. For 180 deg phase shift, low-high peaks occur at $\tau=nP$.

Acknowledgments

The authors acknowledge the contribution received from George Havener, University of Dayton, and Clifford B. Weissman, Wright Aeronautical Laboratories, WPAFB, for the interferometry setup and the holographic material presented. Thanks are extended to Glenn W. Williams, Wright Aeronautical Laboratories, WPAFB, for his help in the data reduction.

References

[1] Bailey, W. H. Jr. and Calarese, W., "Experimental Study of Self-Sustained Shock Oscillations on a Spike-Tipped Body at Mach 3," AFWAL TM-81-53-FIMM, Jan. 1981.

[2] Hankey, W. L. and Shang, J. S., "Analysis of Self-Excited Oscillations in Fluid Flows," AIAA Paper 80-1346, Snowmass, Colo., July 1980.

[3] Shang, J. S., Smith, R. E., and Hankey, W. L., "Flow Oscillations on Spike-Tipped Bodies," AIAA Paper 80-0062, Pasadena, Calif., Jan. 1980.

[4] Harney, D. J., "Oscillating Shocks on Spike Nose Tips at Mach 3," AFFDL-TM-79-9-FX, 1979.

[5] Hankey, W. L., Hunter, L. G., and Harney, D. L., "Self-Sustained Oscillations (Buzz) on Spike Tipped Bodies at Mach 3," AFFDL-TM-79-23-FXM, Jan. 1979.

[6] Reding, J. P., "Fluctuating Pressures on Mildly Indented Nosetips," *Journal of Spacecraft and Rockets*, Vol. 16, Sept.-Oct. 1979, pp. 302-310.

[7] Guether, R. A. and Reding, J. P., "Fluctuating Pressure Environment of a Drag Reduction Spike," AIAA Paper 77-90, Los Angeles, Calif., Jan. 1977.

[8] Demetriades, A. and Hopkins, A. T., "Asymmetric Shock-Wave Oscillations on Spike Bodies of Revolution," *Journal of Spacecraft and Rockets*, Vol. 13, Nov. 1976, pp. 703-704.

[9] Panaras, A. G., "Pulsating Flows About Axisymmetric Concave Bodies," *AIAA Journal*, Vol. 19, June 1981, pp. 804-806.

[10] Calarese, W., Hankey, W. L., and Shang, J. S., "Investigation of Self-Sustained Shock Oscillations on a Spike-Tipped Body at Mach 3," *ASME Proceedings on Computers in Flow Predictions and Fluid Dynamics Experiments*, Washington, D.C., Nov. 1981, pp. 151-156.

[11] Calarese, W., "Flow Visualization and Data Analysis of Self-Sustained Shock Oscillations on a Spiked Body at Mach 3," *ICIASF '81 Record*, IEEE Pub. 81CH1712-9, Sept. 1981, pp. 201-206.

[12] Cassanto, J. M., Monfort, A., and Fehl, C., "An Experiment to Determine the Existence of R/V Nose Tip Transient Shocks," AIAA Paper 76-54, Washington, D.C., Jan. 1976.

[13] Ericsson, L. E., "Flow Pulsations on Concave Conic Forebodies," *Journal of Spacecraft and Rockets*, Vol. 15, Sept.-Oct. 1978, pp. 287-292.

[14] Maull, D. J., "Hypersonic Flow Over Axially Symmetric Spike Bodies," *Journal of Fluid Mechanics*, Vol. 8, Pt. 4, Aug. 1960, pp. 584-594.

[15] Mair, W. A., "Experiments on Separation of Boundary Layers on Probes in Front of Blunt-Nosed Bodies in a Supersonic Stream," *Philosophical Magazine*, Vol. 43, 7th Ser., July 1952, pp. 695-716.

[16] Kabelitz, H. P., "Zur Stabilitat geshlossener Grenzschichtablosegebiete an Konishen Drehkorpern bei Hyperschallanstromung," DLR FB 71-77, July 1971.

[17] Calarese, W. and Hankey, W. L., "Modes of Shock Wave Oscillations on Spike-Tipped Bodies," AIAA Paper 83-0544, Reno, Nev., Jan. 1983.

[18] Rayleigh, Lord, "On the Stability or Instability of Certain Fluid Motion," *Scientific Papers*, Vol. 1, Cambridge University Press, Cambridge, U.K., 1880, pp. 474-484.

[19] Clark, G. F., "Trisonic Gasdynamic Facility User Manual," AFWAL-TR-82-176-FIMM, April 1982.

[20] MacCormack, R. W., "Numerical Solutions of the Interaction of a Shock Wave with Laminar Boundary Layer," *Lecture Notes in Physics*, Vol. 8, 1971, p. 151.